Electronic Journal of Structural Engineering

Original Article

Cite this: DOI:10.56748/ejse.25665

Received Date: 19 July 2024
Accepted Date: 8 January 2025

1443-9255
https://ejsei.com/ejse
Copyright: © The Author(s). Published by Electronic Journals for Science and Engineering International (EJSEI).
This is an open access article under the CC BY license. https://creativecommons.org/licenses/by/4.0/

Optimizing Structural Connections: Finite Element Analysis of Extended End Plates and Bolt Dynamics

Fatimah De'nan[a*], Nor Salwani Hashim[a], Nurul Ain Abd Wahab[a]
[a] School of Civil Engineering, Engineering Campus, Universiti Sains Malaysia, 14300 Nibong Tebal, Pulau Penang, Malaysia
*Corresponding author: cefatimah@usm.my

Abstract

This study analyzed the connection using finite element (FE) simulations and nonlinear analysis to determine its moment resistance and mode of failure. In this work, FEA (finite element analysis) is employed to analyze the triangular web profiled (TRIWP) steel section as a beam element and extended end plate connection. The connection model has been developed with different thicknesses of extended end plate, beam flange, and beam web, and these parameters were analyzed to determine the relationship between all three cases with the failure connections and moment-rotation curve. Furthermore, the results obtained from the analysis of using extended end plate connections have been compared with previous studies where flush end plate connections are used to compare the behavior of the two end plates' connections. Twelve LUSAS analysis models were used, varying parameters such as the thickness of the flange beam, web beam, and end plate. Results indicated that an increased end plate thickness led to a higher moment resistance. A comparison of the moment resistance between the extended end plate and flush end plate connections, from a previous study, showed a difference of 48%. This finding is attributed to the extended end plate's ability to sustain a higher moment compared to the flush end plate. Therefore, the extended end plate connection is stronger than the flush end plate connection. Failure modes showed that buckling occurred at the top flange, which was similar for both types of connections. The use of a triangular shape is used to create contrast as this is prominent from the other shapes used commonly in web design.

Keywords

Connection, Finite element analysis, End plate, Buckling

1. Introduction

The connection is a crucial aspect of structural steelwork, as the forces supported by structural members are transferred to other parts through it. The relationship between the rotation and joint moment of the connected member can be found through a moment-rotation curve (M-ϕ) (Tahir and Hussein, 2008). Structural steel is often used as a construction material due to its desirable attributes, such as strength, stiffness, toughness, and ductility. Components such as girders, beams, floor plates, trusses, columns, and purlins are typically connected using fasteners such as nuts, washers, bolts, and shear connectors (SCI, 1995). The connection not only affects the total cost of structures (Murray and Sumner, 2003) but also influences the performance of the entire structure (Chen and Richard, 2003) and facilitates the strengthening of the structure (Xu et al., 2017).

Recently, much research and development works have been done on steel composites due to their advantages as a structural material compared to steel or timber. Steel sections can sustain earthquake loads, making them an important construction material in seismic regions (Adey et al., 2000). After the Northridge earthquake in January 1994, no collapses of steel-framed buildings were found, despite the ground motion failure (Chen and Yamaguchi, 1996). However, major damage was found in most frame buildings, which generally involved the cracking of welded connections.

In the early 1960s, end plates were used for beam-splice and beam-to-column connections for moment resisting purposes. In the United States, this connection was primarily used in pre-engineered metal buildings until the mid-1980s (John and Ryan, 1999). End plate connections are mainly used to build light story buildings and generally have adequate behavior and reasonable cost, which can be achieved using the split tee connection. Nowadays, extended end plate connections and flush end plate connections are mostly available in the market (Tiew, 2010; Al Fakih et al., 2018). Fig. 1 show types of end plate connections that are often used to connect beams to columns.

The substantial moment from the beam to columns is transferred by using an extended end-plate connection. The beam to column welded connection is more rigid than the bolted beam to column connection due to its higher stiffness and moment resistance. Partial strength connection is the most popular type of end-plate connection. This can be achieved by using higher quality welds than with field-welded connections since the welding for these connections is done under controlled conditions (Adey et al., 2000). However, when high moments arise, the use of extended end-plate connections is considered (Hassan et al., 1997).

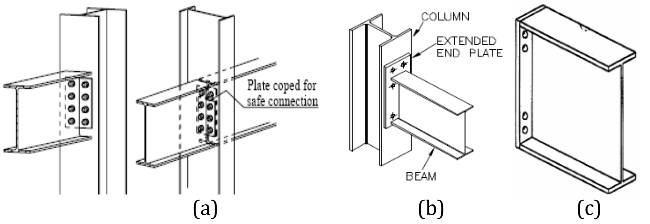

Fig. 1 Type of end plate connection a) Bolted end plate b) Bolted extended end plate c) Flush end plate, (Ioan et al., 2021; Luo et al., 2020; Khonsari et al., 2022).

In particular, by using an appropriate location and number of bolts, stiffeners in the column panel, and an appropriate end-plate geometrical configuration and thickness, both rotational stiffness and flexural resistance can be improved (John and Ryan, 1999). Besides that, a 20% increment of direct force for the bolt forces on the tension flange of extended end-plate connections is observed (Grundy et al., 1980). Thus, due to this behavior, the extended end-plate connections are identified as partial strength connections (Tahir and Hussein, 2008). An increment in moment resistance and stiffness of the connections is found depending on the geometric parameters such as the number and size of bolts, the use of deeper beams, and the thickness of the end plate (Bahaz et al., 2018). For this type of connection, the neutral axis mostly governs the section capacity (Ioan et al., 2021).

For the stiffening bolted end-plate connections, a notable increase in initial stiffness and moment resistance capacity is observed but leads to a reduction of connection ductility (Abidelah et al., 2012; Shi et al., 2006). About a 60-90% increment of ultimate moment is observed by the use of an extended endplate with rib stiffener, and about 140% of initial stiffness is more than those of the flush-type connection (Ismail et al., 2016). Up to a 30% increase in endplate bending capacity is achieved by using end-plate stiffeners in thin plate connections (Dessouki et al., 2013).

Besides that, the introduction of corrugated web contributes to the use of thin plates without stiffeners, which can improve aesthetics appearance. The use of larger thickness can be avoided, thus contributing to the lower weight and cost of the beam (Chan et al., 2002). In Europe, girders with corrugated web were extensively used for steel buildings and highway bridges since the early 1960s (Abbas, 2003). Two steel flanges welded to a steel web in a corrugated profile are known as a corrugated web steel I-girder. The web profile could be trapezoidal, sinusoidal, rectangular, triangular, or any other web shape (Abbas et al., 2006). The use of corrugated steel web is believed to enhance shear buckling strength, reduce the size of the component, and eliminate the need for transverse stiffeners (Moon et al., 2009).

Previously, an analysis of corrugated web profiles was performed to investigate the strength of multi-web beams (Chan et al., 2002; Khalid et al., 2004). This involved the effects of corrugation radii on the beam's strength, where larger corrugation radii achieved higher moment capacity. The reduction in the weight of the beam could be observed when using the maximum size of corrugation radius for vertically corrugated web. Recently, the behavior of tubular flange and corrugated web subjected to shear, bending, and axial compression was described (Wang, 2003). The present parametric study shows that the value of the shear force acting on the connection has a significant effect on the connection stiffness (ElSabbagh et al., 2019). For the plastic hinge location, corrugated webs increase plastic stability without any brittle fractures and provide large plastic rotation in this location. The mechanical properties of the Trapezoid Web Profile (TWP), such as shear buckling strength, moment capacity, axial buckling, flange capacity, and deflection, have been clearly discussed (De'nan and Hashim, 2011 – Barmaki et al., 2020).

The analysis only covered the extended end-plate connection with TRIWP steel section using software LUSAS 14.0. Several thicknesses of the extended end plate, beam flange, and beam web will be analyzed. The model contains a triangular web profile steel section beam connected to a Universal Column (UC) section column by means of an extended end-plate connection. The comparison of the results will be done by comparing the moment resistance for different thicknesses of the end plate, beam flange, and beam web from the previous study.

A previous study may have provided insights into the behavior of extended end-plate connections in certain conditions, it's crucial to recognize that structural behavior can be highly sensitive to various parameters. In this study, the analysis focuses specifically on the extended end-plate connection using TRIWP steel sections, which presents a unique configuration that may exhibit distinct behavior compared to the previous study's findings. Secondly, the consideration of different thicknesses of the extended end plate, beam flange, and beam web introduces a parametric study that examines a broader range of scenarios. This approach enhances the comprehensiveness and applicability of the findings, allowing for a more detailed understanding of how different geometrical factors influence the connection's performance. Moreover, the utilization of a specialized software like LUSAS 14.0 offers the opportunity to conduct more advanced and precise simulations, potentially capturing intricate nonlinear behavior and interactions that might not have been fully explored in the previous study. Additionally, the focus on a triangular web profile steel section beam connected to a Universal Column (UC) section column introduces another layer of complexity. This combination may lead to different load distribution patterns and failure mechanisms compared to the previous study's setup, necessitating a dedicated analysis to comprehensively evaluate the connection's behavior. The intended comparison of results with the previous study is valuable for cross-validation and verification purposes. It helps establish the consistency of findings across different studies and further refines our understanding of how variations in end plate, beam flange, and beam web thicknesses impact moment resistance.

2. Methods

In this work, FEA (finite element analysis) is employed to analyze the triangular web profiled (TRIWP) steel section as a beam element and extended end plate connection. The connection model has been developed with different thicknesses of extended end plate, beam flange, and beam web, and these parameters were analyzed to determine the relationship between all three cases with the failure connections and moment-rotation curve. Furthermore, the results obtained from the analysis of using extended end plate connections have been compared with previous studies where flush end plate connections are used to compare the behavior of the two end plates' connections.

2.1 Configuration of the Connection

Twelve finite element models of extended end plate connections were used and compared to observe their behavior. All the required parameters for modelling the connection for the column and beam are given in Table 1. The typical FEA models are shown in Fig. 2, and the geometries of the section models are based on the typical size of Perwaja Steel Section (PSS).

2.2 Finite Element Analysis

This study investigates the behavior of steel extended end-plate moment connections under static load. Initially, different methods of modeling and bolt element numbers were created using LUSAS software to finalize the arrangement of elements and mesh. Parameters for other parts of the model, such as the beam, column, and end plate, including section, elements, and meshing, were similar. The model consists of a TRIWP beam, extended end plate, bolt, and column, with the entire dimension, connection parameters, and modeling process based on a previous study (Tahir et al., 2008). The structure was modeled using a combination of 3D thick shell element (QTS4), continuum element (HX8M), bar element (BRS2), and joint element (JNT4). The procedures were the same for all 12 models, except for the extended end plate, flange beam, and web beam, which differed in thickness. The beam-to-column connection consists of four major components: the extended end plate, beam, column, and bolt.

Table 1. Properties of beam to column extended end plate connection

Section	Column (mm)		Beam (mm)		Extended End Plate (mm)	Bolt
Case 1	(2003200363.8 UKC)		(4503200)		(6503200)	M20 grade 8.8
	Flange	Web	Flange	Web	Thickness	
	12	8	7	4.5	10 12 15 20	
Case 2	12	8	7 10 12 14	4.5	20	
Case 3	12	8	7	4.5 8 10 12	20	

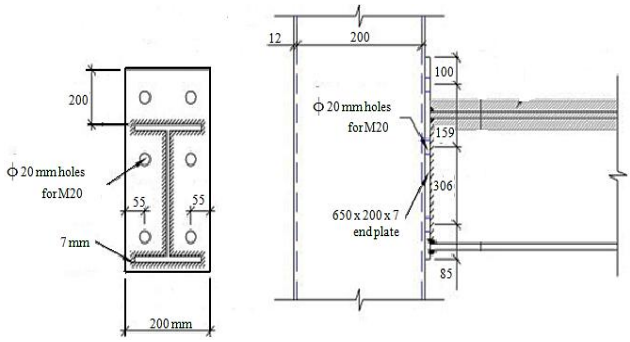

Fig. 2 Typical arrangement for extended end plate

Model geometry

In the context of the analysis, the extended end plate was generated using HX8M elements based on volume geometry. The end plate's thickness, a pivotal parameter influencing connection behavior and result accuracy, was varied across four different dimensions: 10 mm, 12 mm, 15 mm, and 20 mm. Bolt holes were incorporated into the solid plate for bolt installation, further enhancing the end plate model's realism. The beam, with a depth and width of 450 mm and 200 mm, respectively, featured controlled web and flange member thicknesses to explore their influence on connection behavior. A beam length of 1500 mm was adopted for the analysis. The web was designed using surface geometry, while the beam flanges employed volume geometry, considering the web as less critical. Welding the end plate and beam models as a single member ensured cohesive behavior, sharing the same nodes. The column, with a fixed height of 3000 mm and dimensions of 200×200 mm, respectively, according to Perwaja, Malaysia Steel Section (PSS) which is maintained uniform parameters across all models. The column web was modeled using volume geometry, and the flange was modeled using surface geometry. The bolt holes were also modeled in the web. To reduce the number of elements and speed up the analysis, surface geometry was used to model the column flange. As long as the real geometric parameters were assigned to the surface, this would not reduce the accuracy of the result (Tai, 2005). Volume and surface geometry were employed to model the column web and flange, respectively, along with bolt holes in the web. Bolts and nuts were represented by grade M24 and grade 8.8 components, modeled as a single unit using volume geometry. Bolt bodies, assigned to a 245mm2 tensile stress area, employed line geometry and automatic meshing. The bolt heads and nuts were simplified into rectangular shapes without affecting accuracy, given their constant surface areas and stress levels, as per the equation σ=P/A (Ouh, 2009).

Element Types and Meshing

As stated earlier, LUSAS element library contains about 100 elements covering ten element groups. Element types HX8M, QTS4, BRS2, and JNT4 were chosen to model the various components of the extended end plate connections.

Material nonlinearity is a linear stress-strain relationship caused by strain hardening and plastic yielding. Steel is categorized as a ductile material that displays nonlinear material properties. For the elastic dataset, elastic isotropic elements with a Poisson's ratio of lateral to longitudinal strain of 0.3 and Young's Modulus of Elasticity of 2.05 x 105 N/mm2 were used. Joint material (JNT4) was assigned to the contact lines between end plates as shown in Fig. 3. The joint type was spring stiffness (K), 1000 N/mm2. For contact lines between bolts and nuts, the K value is 10 000 N/mm2. The plastic dataset was defined as shown in Table 2.

Table 2. Plastic Dataset

	Bolt and shank	Beam, column, end plate
Initial uniaxial yield stress (N/mm^2)	560	300
Hardening gradient slope	20 000	1 000
Plastic strain	200	100

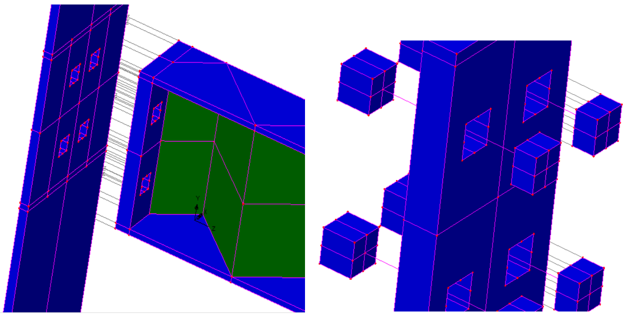

Fig. 3 Joint contact for endplate to column and bolt to endplate

The figure in Fig. 4 presents the maximum nodal displacement for eight models, each featuring varying numbers of elements and nodes. A consistent trend is observed where the displacement values decrease progressively from Model 1 to Model 8. Convergence is attained when the element count reaches 2228, leading to the utilization of 20 mm elements for the entire analysis.

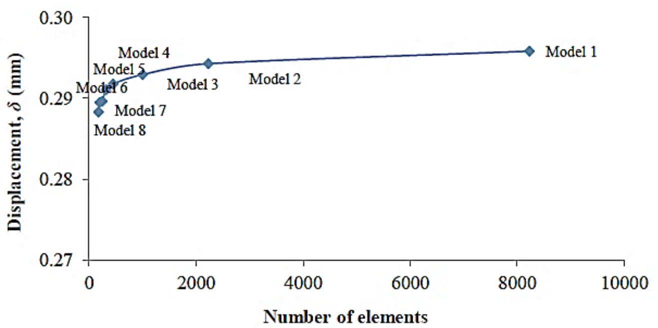

Fig. 4 Graph of maximum nodal displacement

Figure 5 displays the boundary conditions applied in the model analysis. The top and bottom ends of the column were fixed, and both translation and rotation were constrained in all directions.

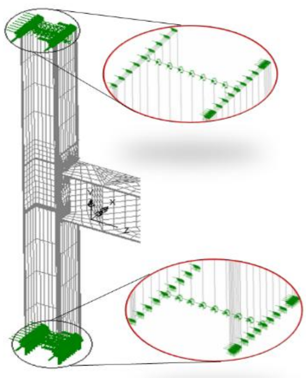

Fig. 5 The Boundary Conditions of the Model

In the nonlinear analysis, a concentrated load of 500 N was applied at a location 1300 mm from the end plate. To achieve the required range of bending moments, the total load factor was increased from 1.0 to 200.0.

2.3 Determination of Moment and Rotation Value

To plot a moment rotation curve, the moment and rotation value were computed from the raw data. Point C is located at the center of the column web, where the distance from half of the column height from the base is 412.5 mm. Point B is located at the neutral axis of the beam with a horizontal distance of 320 mm from the external surface of column flanges.

The rotation of the connection was calculated based on the displacement of the beam in the Y direction and the displacement of the column in the Z direction. Using the displacement values, the rotations of the two nodes (Yb and Yc) were calculated using the Pythagoras Theorem.

The calculation procedure for determining the connection rotation (Yj) involves several steps. The rotation value (Φj) is obtained by subtracting the beam rotation (Φb) from the column rotation (Φc), as expressed in equation (1). The beam rotation (Φb) is calculated using the arctangent function applied to the ratio of vertical displacement (Δy) divided by 320, as given by equation (2). Similarly, the column rotation (Φc) is determined using the arctangent function applied to the ratio of horizontal displacement (Δz) divided by 412.5, as specified in equation (3). The applied moment (M) is then computed using the following formula: M = Total load factor × 0.5 × 1.32. In this equation, M represents the applied moment in kNm. The load factor is considered in the calculation, and the value 0.5 represents the applied load in kN, which acts at a distance of 1.32 meters from the column face.

The calculation procedures for connection rotation (Yj) are as follows.

$$\Phi_j = Y_b - Y_c \qquad (1)$$

$$Y_b = \mathrm{Tan}^{-1}(\Delta_y/320) \qquad (2)$$

$$Y_c = \mathrm{Tan}^{-1}(\Delta_z/412.5) \qquad (3)$$

where;

Y_b = Beam rotation
Y_c = Column rotation
Φ_j = Rotation
Δ_y = Vertical displacement
Δ_z = Horizontal displacement

The displacement based at certain nodes can be obtained from LUSAS software based on the raw data of corresponding increment of loading. However, LUSAS software cannot directly produce moment rotation curve. Therefore, the results of displacements at appropriate nodes for each load increment given by LUSAS in 2004 had to be extracted and computed manually. To develop the moment rotation curve (M-⍰), the deflection of the beam and column in the x and y axis must be obtained from the analysis. The value for moment resistance (MR) was determined from the plotted (M-⍰). To form a plateau, the straight line of the non-linear region is drawn as a curve. This intersection method of moment rotation curves is known as a "knee joint" (Nigel, 1995; Saggaff, 2006).

The design of modelling was accomplished through finite element software. Twelve models were constructed using LUSAS software, with three cases: Case 1 studied an extended end plate with different thickness; Case 2 studied a flange beam with different thickness, and Case 3 studied different thickness of TRIWP beam. The aim of this work is to determine the rigidity of beam (rotational stiffness) and strength (moment resistance) of the TRIWP beam–column connection, depending on the thickness of the material such as end plate, number, and size of bolts.

The total load factors, displacement at z axis for node C, and displacement of y axis for node B were obtained directly from the analysis. The value for the moment (M) and rotation (θj) for each model were calculated from the finite element result. The outcome of this study is as follows:

I. The moment rotation curve obtained from LUSAS analysis for all the three cases.
II. The moment resistance value (MR) obtained from the moment rotation curve of LUSAS analysis for all the three cases.
III. By using extended end plate and triangular web profiled (TRIWP) beam section, the mode of failure for the beam column connection were obtained from the analysis
IV. Appropriate thickness of extended end plate, triangular web profiled (TRIWP) beam section and flange beam for extended end plate bolted connection for triangular web profiled (TRIWP) beam steel section.

2.4 Material and Geometric Nonlinearity

The stress-strain constitutive relationships are nonlinear. This behavior, such as the elasto-plastic behavior in metal when loaded past the yield point and creep of metals at high temperatures, explains that the linear assumption can be used up to the yield point. However, after the yield point, a significant error occurs if the linear theory is used because the stress-strain relationship has become nonlinear.

Geometric nonlinearity occurs when the changes in the geometry of a structure due to its displacement under loading are taken into account in the analysis of its behavior. The change in geometry affects both equilibrium and kinematics. In geometric nonlinearity, the equilibrium equations consider the deformed shape, whereas in linear analysis, the equilibrium equations consider the undeformed shape. Geometric nonlinearity does not always mean large displacements. Moreover, large displacements are not always associated with large strains.

3. Results

In this section, different factors were considered to investigate the effect of connection behavior. The variable parameters were deliberated as well as the thickness of the extended end plate and thickness of Triangular Web Profiled (TRIWP) Beam were studied. The boundary condition, material models and the geometry, i.e. cross-section and lengths of column and beams were kept constants.

3.1 Effect of Extended End Plate Thickness

The moment–rotation graph (Figure 6) is relatively constant in the elastic stage that led to the loading process into plastic phase (the loading curves would create fluctuations). This was due to the certain steel components have reached their yield limit. Besides that, the different deformation on each analysis was maybe due to the random plastic deformation in the steel section. Therefore, to eliminate the differences, the data of each analysis were averaged before comparing with the finite element analysis (FEA) results.

In case 1, the study analyzed four models of extended end plates with varying thicknesses. The thicknesses considered were 10 mm, 12 mm, 15 mm, and 20 mm. The results showed that the moment resistance (MR) value for the extended end plate with a 10 mm thickness was 75 kNm, while for the rest of the models, the value was 85 kNm. The findings suggest that the thickness of the extended end plate has a significant impact on the moment rotation curve and its moment resistance value. Generally, as the thickness of the end plate increases, the MR value also increases. This relationship can be attributed to the increased stiffness of the connection with a thicker end plate, leading to an increased moment resistance. When the end plate is thicker, it provides additional support to the beam, which leads to a more rigid connection. A stiffer connection can resist greater moments before failure. This is because the increased thickness of the end plate allows for a larger distribution of stress over a larger area, reducing the localized stress on the bolts and increasing the load-bearing capacity of the connection. In addition, a thicker end plate increases the overall cross-sectional area of the connection, which can also contribute to an increased moment resistance. Therefore, a thicker end plate can provide greater stability and strength to the connection, leading to an increased moment resistance. A study by Daneshgar and Mohammadi (2018) on the behavior of extended end plate connections reported that increasing the thickness of the end plate led to an increased moment resistance. Similarly, a study by Alnahhal and Al-Safary (2016) investigated the effect of end plate thickness on the moment resistance of bolted connections and found that thicker end plates led to a higher moment resistance.

The observed failure mechanism resulted from a combination of factors, including the deformation of bolts and beam flange, as well as bending at the end plate. The analysis revealed that for each thickness of the extended end plate, the deformations witnessed were primarily due to a combination of local buckling and displacement at the top flange. This behavior is evident in Figures 7(a) and (d), depicting the deformed shapes of the extended end plate with thicknesses ranging from 10 mm to 20 mm, respectively. As the thickness of the extended end plate increases, the deformations also increase, which can be attributed to its role in transferring and distributing the loads within the connection. Consequently, the selection of the appropriate thickness for the extended end plate becomes a critical aspect of the design process. Opting for a plate that is too thin may compromise its ability to withstand high loads, while opting for a plate that is excessively thick might lead to excessive deformation in the connected beam due to stiffness imbalances.

Recent studies have also highlighted the importance of selecting the appropriate thickness of the extended end plate. For example, in a study by Wang et al. (2020), it was found that the thickness of the extended end plate significantly affected the stiffness and strength of the beam-to-column connection. Similarly, in a study by Yin et al. (2021), it was reported that the thickness of the extended end plate played a critical role in the connection's resistance to bending and shear forces. The findings of this study align with recent work that has emphasized the pivotal role of selecting the suitable thickness for the extended end plate. For instance, Wang et al. (2020) conducted a study that demonstrated the significant impact of the extended end plate's thickness on both the stiffness and strength of beam-to-column connections. Similarly, in another study by Yin et al. (2021), it was highlighted that the thickness of the extended end plate has a critical influence on the connection's capacity to withstand bending and shear forces. These results corroborate the present study's observations regarding the deformation and failure mechanisms of the connection under varying thicknesses of the extended end plate. It underscores the necessity for thoughtful consideration when determining the appropriate thickness of the extended end plate during the design process, ensuring that the connection can deliver optimal performance while meeting the intended structural requirements.

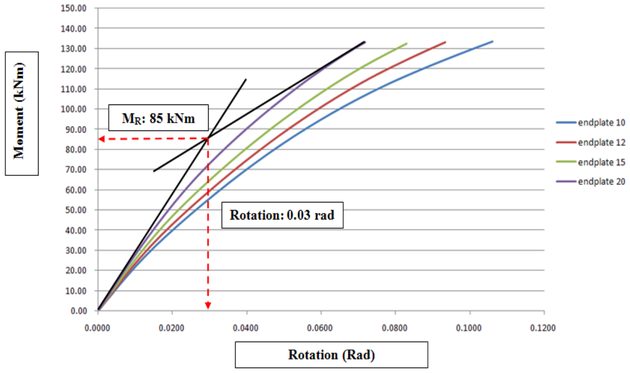

Fig. 6 Moment rotation curve for different thicknesses of extended end plate

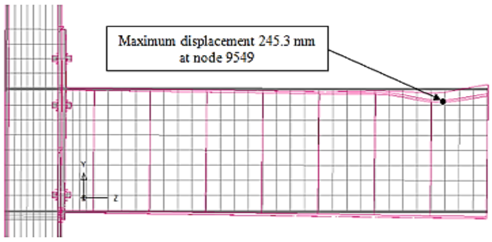

(a) 10 mm thickness

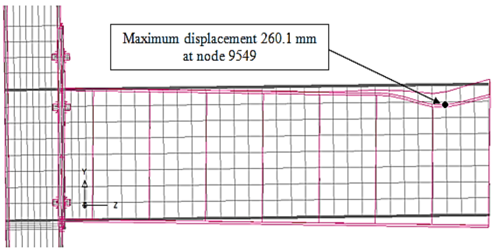

(b) 12 mm thickness

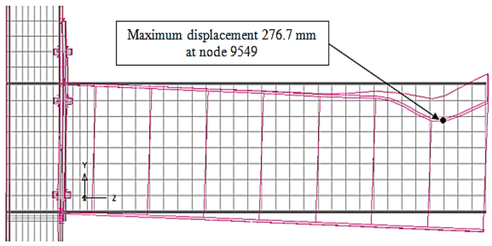

(c) 15 mm thickness

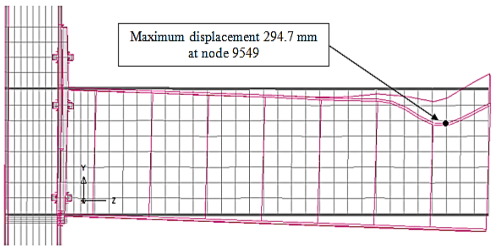

(d) 20 mm thickness

Fig. 7 Deformed shape of various extended end plate thickness

3.2 Effect of Beam Flange Thickness

In this case, the effect of the beam flange thickness on the beam to column connection behavior was examined. Four cases of beam flange thickness of 7 mm, 10 mm, 12 mm, and 14 mm were used to compare the moment rotation. Only beam flange thickness was changed while other parameters remained constant. Figure 8 shows the moment rotation (M-θ) curve with different beam flange thicknesses and the moment resistance value for all graphs, in this case, is 95 kNm. As a summary, the moment rotation curve was not affected by the thickness of the beam flange.

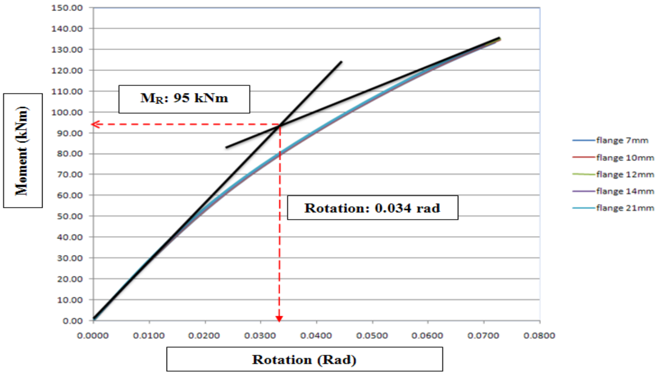

Fig. 8 Moment Rotation Curve for Different Thickness of Beam Flange

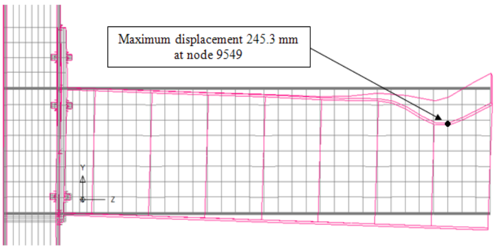

(a) 7 mm thickness of Beam Flange

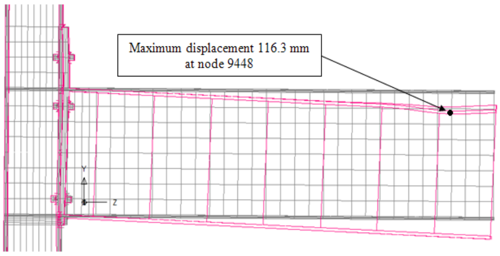

(b) 10 mm thickness of Beam Flange

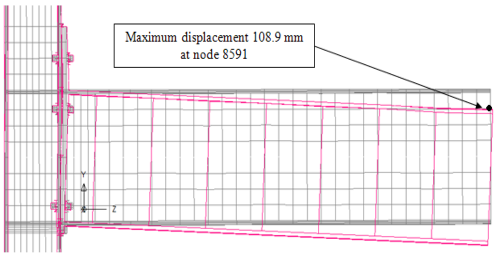

(c) 12 mm thickness of Beam Flange

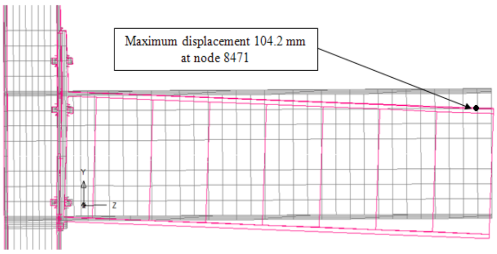

(d) 14 mm thickness of Beam Flange

Fig. 9 Deformed shape of various beam flange thickness

The deformation behavior of the models with different thicknesses of beam flange was investigated. For the models with thicknesses of 7 mm and 10 mm, the deformation was a combination of displacement and local buckling, which occurred at the top flange of the beam. In contrast, for the models with thicknesses of 12 mm and 14 mm, only displacement occurred. The maximum displacement values were observed at the location of the applied load. This is due to the thickness of the beam flange was sufficient to prevent local buckling. Local buckling typically occurs when the width-to-thickness ratio of the plate is too high, resulting in a reduction of the plate's stiffness and strength. Therefore, the increased thickness of the beam flange in the 12 mm and 14 mm models reduced the width-to-thickness ratio, preventing local buckling from occurring.

As a result, the maximum displacement values observed in the 12 mm and 14 mm models were mainly due to the deformation caused by the applied load. Since the thickness of the beam flange was sufficient to resist local buckling, the beam was able to deform in a purely elastic manner, without undergoing any plastic deformation or buckling. Therefore, the maximum displacement values were observed at the location of the applied load, which is the point where the beam experiences the highest stress and deformation.

Figures 9(a) to (d) display the deformed shapes of the 10 mm and 12 mm thicknesses of the beam flange, respectively. Based on the maximum displacement values, it can be concluded that as the thickness of the beam flange increases, the displacement value also increases. Based on the maximum displacement values observed in the experiment, it can be concluded that when the thickness of the beam flange increases, the displacement value also increases. This can be explained by the fact that increasing the thickness of the beam flange increases the stiffness and strength of the beam, which allows it to resist deformation and displacement more effectively. This phenomenon can be attributed to the inherent connection between flange thickness, stiffness, and strength of the beam. As the beam flange thickness increases, the beam becomes stiffer and exhibits enhanced structural integrity, enabling it to more effectively resist deformation and displacement.

However, it is important to note that the deformation of the beam flange must also be taken into consideration, as it can affect the deformation of the endplate around the highest bolt holes. This observation aligns with the findings of Pan et al. (2018), where it was demonstrated that the deformation of the endplate around the highest bolt holes was not solely a result of beam web tension but was significantly influenced by the behavior of the beam flange. In their study, they emphasized that the deformation in the vicinity of the highest bolt holes was primarily due to the interaction of multiple factors, including the tension of the beam web and, notably, the behavior of the beam flange. This resonates with the present study's conclusion that variations in beam flange thickness can significantly impact the connection's deformation behavior. Therefore, the increased stiffness and strength resulting from thicker beam flanges contribute to enhanced resistance against deformation and displacement, thus influencing the overall performance and behavior of the connection.

3.3 Effect of Triangular Web Profiled (TRIWP) Beam Thickness

Figure 10 shows four graphs of moment rotation from four models with different thicknesses of TRIWP beam. The graphs display the moment rotation of the TRIWP beam with thicknesses of 4.5 mm, 8.0 mm, 10.0 mm, and 12.0 mm together in one figure. All the graphs have the same moment resistance (MR) value of 82 kNm, obtained from the moment rotation curve, with a rotation of about 0.027 rad. Interestingly, the changes in TRIWP beam thickness did not significantly affect the MR value, and as a result, the graphs show little difference in the thickness of the beam web. This is likely due to the fact that the beam web does not play a significant role in resisting bending moments in the beam, and most of the resistance to bending moments comes from the beam's flanges.

In this case, all modes of deformed were the same. Although the thicknesses of the beam web varied, the deformations were a combination of displacement and local buckling, which occurred at the top flange of the beam for all thicknesses. The maximum displacement values obtained from the analysis increased as the thickness of the beam web increased. Figures 11(a) to (d) depict the deformed shapes of 10 mm and 12 mm thicknesses of triangular web profiled (TRIWP) beams.

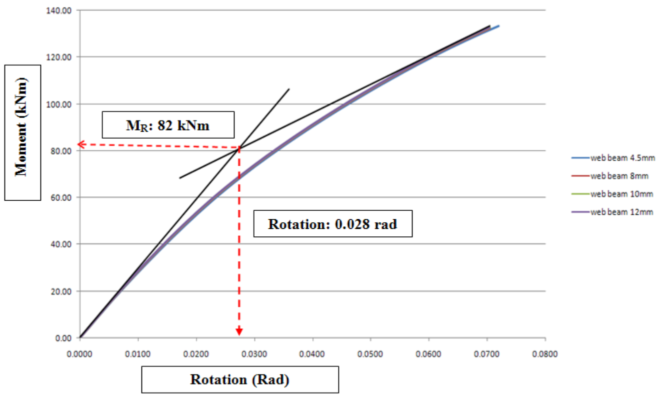

Fig. 10 Moment rotation curve for different thickness of TRIWP beam

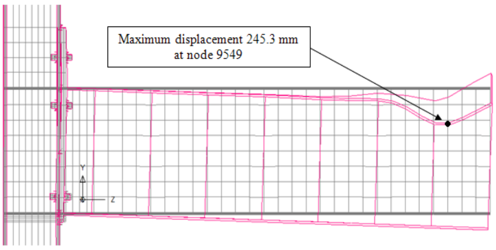

(a) 4.5 mm thickness

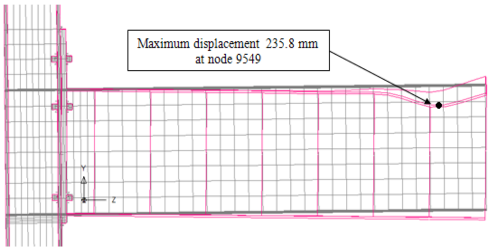

(b) 8 mm thickness

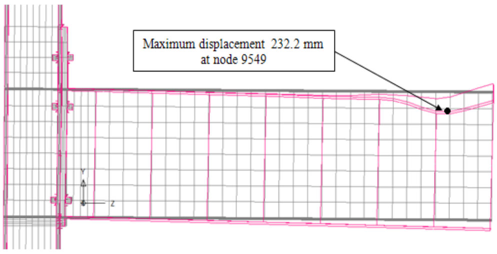

(c) 10 mm thickness of Beam Web

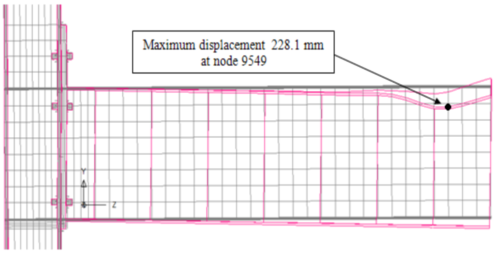

(d) 12 mm thickness of Beam Web

Fig. 11 Deformed shape of various beam web thickness

From each deformed section, most of the yielding is due to the moment transfer in this area. Therefore, the flange section in the area adjacent to the end plate has not yielded. However, it can be observed that the yielding in the flange section becomes more apparent when the thickness of the web increases.

3.4 Comparison of performance of beam-to-column connection using extended end plate and flush end plate

The parametric studies involved analyzing the moment-rotation (M-ϕ) curves of each connection, which are described by three major characteristics: moment resistance, displacement, and rotation capacity. Figure 12 depicts the moment-rotation graph for the beam to column connection using an extended end plate connection. The graph shows a moment resistance of 60 kNm and a rotation capacity of 20 rad using an extended end plate.

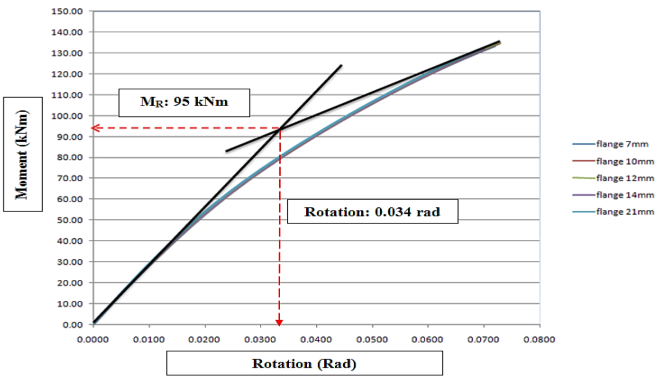

Fig. 12 Graph of Moment Rotation by Using Extended End Plate

The moment resistance obtained from the graph is 31 kNm, and the rotation for using the extended end plate is 70 rad. To reduce the rotation capacity of each connection, it is suggested to use the stiffened connection. This was applied by Osman and Mourad in 2021, where the presence of additional end-plate rib stiffeners improved the maximum pressure that can be sustained by the connection, considering the same blast duration. Furthermore, using end-plate stiffeners and side stiffeners in extended endplate bolted connections increases both the load carrying and moment carrying capacity. When a concentrated load is applied to the connection, the stiffeners help distribute the load more evenly across the connection, reducing localized stresses and increasing the load carrying capacity. Additionally, the increased stiffness provided by the stiffeners helps to resist deformation and rotation of the connection under load, which increases the moment carrying capacity.

Specifically, the use of end-plate stiffeners increases the moment carrying capacity by 15% when compared to unstiffened connections because the stiffeners help to reduce the deformation of the connection under load, which in turn reduces the amount of bending in the end plate. This reduction in bending allows the end plate to carry a higher moment without yielding or failing, thus increasing the moment carrying capacity of the connection. According to Sathian and Geetha in 2020, there was no increase in bending in the outer part of the end plate, even though there were still gaps between the end plate near the beam tension flange and the column flange. Furthermore, extended end-plate connections have gained popularity in modern construction due to their potential for enhancing structural performance and efficiency. As these connections deviate from traditional designs, understanding their behavior becomes essential to ensure that they meet safety standards and contribute positively to the overall structural integrity.

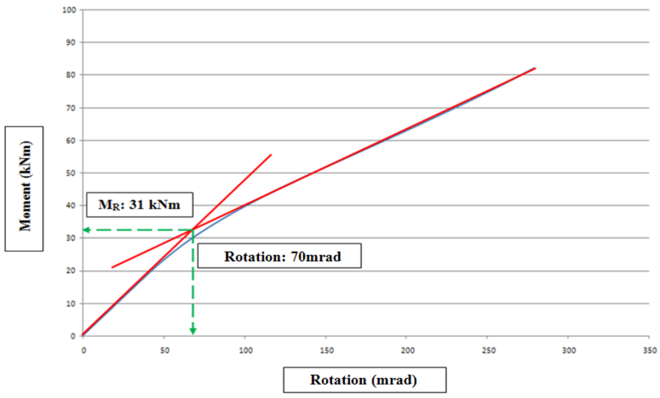

Fig. 13 Graph of Moment Rotation by Using Flush End Plate

Based on the results, the extended end plate connection showed a higher moment resistance value compared to the flush end plate connection. However, it was found that the extended end plate connection had a lower rotation value compared to the flush end plate connection. These findings are consistent with previous studies by Hassan et al. (1997). The difference in moment resistance value between the two end plate connections was 48%. Therefore, it can be concluded that the extended end plate is stronger than the flush end plate connection. Moreover, the percentage difference in rotation between the two end plates was 71%, indicating that the flush end plate connection was easier to rotate under high loads. In conclusion, the extended end plate is the best option for the beam to column connection, as also agreed upon by Yang and Zhou (2019). However, the thickness of the end plate must be considered, as the plastic moment of the beam must be lower than the moment capacity of its section (Gholampour et al., 2014). Modified blind bolts (Hollo-Bolt) in the panel zone have also been shown to overcome moment-resisting problems for bolted connections between concrete-filled hollow section columns and open section beams (Wang et al., 2020). Furthermore, recent studies on the initial rotational stiffness of minor-axis flush end-plate connections showed that the end plate significantly affects the minor-axis connection performance, and the bending stiffness has a significant effect on the entire connection rotational stiffness (Pan et al., 2018).

Figure 14(a) shows the Von Mises stress contour on solid elements contributed by the end plate, beam flange, bolt head, and connecting column flange. On the other hand, Figure 14(b) shows the stress contour on the beam web, column web, and far end column flange, which was modeled as a thick shell element. The stresses on solid elements and thick shell elements cannot be plotted in the same graph since they have different degrees of freedom. In this plot, the stress distribution is represented by a color map, where each color corresponds to a specific stress level. The highest stress levels are typically indicated by warmer colors, such as red or orange, while lower stress levels are indicated by cooler colors, such as blue or green.

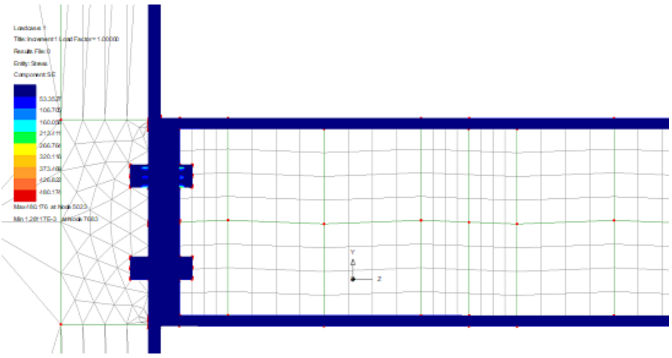

(a)

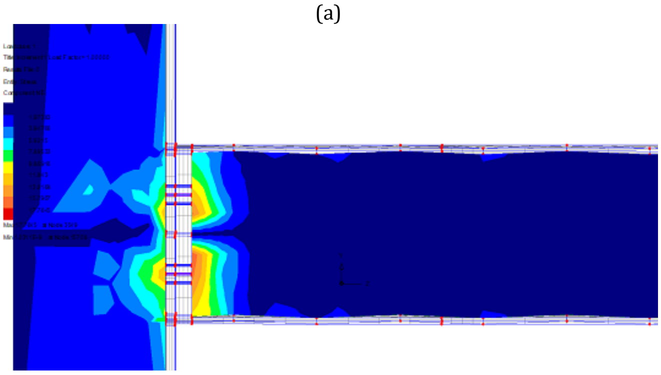

(b)

Fig. 14(a)-The plot of von Mises stress for end plate, bolt and connecting column flange (b)-The plot of von Mises stress for column and beam web and far end column flange.

Additionally, the choice of the TRIWP steel section is significant, as it represents a specific type of beam geometry that might exhibit unique behavior when combined with extended end-plate connections. This study, therefore, seeks to bridge the knowledge gap regarding the interaction between TRIWP beams and extended end-plate connections, which could have implications for the design and optimization of such connections in practical construction projects.

In summary, this study is necessary to expand our understanding of the moment resistance behavior of extended end-plate connections with TRIWP steel sections, utilizing advanced numerical analysis tools. The insights gained from this research can inform better design practices, improve structural performance, and contribute to the safe and efficient use of these connections in real-world construction applications.

4. Conclusion

The behavior of the beam-to-column connection using an extended end plate and TRIWP beam steel section was analyzed using the finite element method. The connection's capacity is mainly affected by geometric aspects such as the number of bolts, thickness and size of the end plate, size of the column and beam. In this study, the end plate thickness and beam flange and web thickness were found to significantly affect the connection's stiffness and moment resistance (MR). However, the flange and web thickness did not have a significant effect on the MR value. The MR value only changed with a change in the thickness of the extended end plate. Comparing the finite element models using an extended end plate and flush end plate (from a previous study), the moment resistance (MR) values were different. The extended end plate can sustain a higher load compared to the flush end plate, with the MR value and rotation of the extended end plate differing from the flush end plate by 48% and 71%, respectively. Therefore, the extended end plate is more suitable to be used than the flush end plate due to its higher strength (moment resistance) and rigidity (rotational stiffness).

Acknowledgement

We wish to express deepest thankfulness and highest appreciation to Universiti Sains Malaysia for the financial support of the Bridging Grant with project no: R501-LR-RND003-0000 000740-0000

Conflict of Interest

The author(s) declared no potential conflicts of interest with respect to the research, authorship, and/or publication of this article.

References

Tahir, M.M. and Hussein, M.A. (2008), “Experimental test on extended end plate connections with variables parameters”, International journal of Steel Structures, 8(4), 369-381.

Steel Construction Institute, SCI, (1995), "Modelling of steel structures for computer analysis, British Library Cataloguing-in-Publication Data, P148.

Murray, M.T. and Sumner, A.E. (2003), Extended end plate moment connections seismic and wing applications – Steel Design Guide, 2nd ed, American Institute of Steel Construction, Inc.

Chen, W.F. and Richard, L.J.Y. (2003), The civil engineering handbook, Second Edition. Boca Raton: Crc Press Llc.

Xu, X. –l., Lu, Z. –d., Li, L. –z. and Jiang, C. –j. (2017), “Numerical Study on the Local Buckling Behaviour of Bolted Steel Plates in Steel Jacketing”, Advances in Materials Science and Engineering, 1352084, 1-15 https://doi.org/10.1155/2017/1352084

Adey, B. T., Grondin, G. Y. and Cheng, J. J. R. (2000), “Cyclic loading of end plate moment connections”, Canadian Journal of Civil Engineering, 27(4), 683-701, https://doi.org/10.1139/l99-080

Chen, W.F. and Yamaguchi, E. (1996), Spotlight on steel moment frames, Civil Engineering, March.

John, C. and Ryan, Jr. (1999), "Evaluation of extended end-plate moment connections under seismic loading’, Research Report, Faculty of the Virginia Polytechnic Institute and State University.

Tiew, L.Y. (2010), ‘Finite element analysis of trapezoidal web beam to column end plate connection’, Research Report, Faculty of Civil Engineering & Earth resources Universiti Malaysia Pahang.

Al Fakih, K., Chin, S.C. and Doh, S.I. (2018), “Behavior of extended end-plate steel beam to column connections”, The Open Civil Engineering Journal, 12, 250-262. https://doi.org/10.2174/1874149501812010250

Birdean Calin Ioan, Cernescu Anghel, Faur Nicolae1, (2021) “Design Method for Endplate Bolted Connections”, IOP Conf. Series: Materials Science and Engineering 1203 (2021) 022062, 1-12

Liang Luo, Maohua Du, Jian Yuan, Jun Shi, Suhui Yu and Yi Zhang, (2020) “Parametric Analysis and Stiffness Investigation of Extended End-Plate Connection”, Materials, 13(22), 5133; https://doi.org/10.3390/ma13225133

Khonsari, S.V., Nejati, S., Rahdan, M. and Ahmadi, M. (2022), "Behaviour of thin flush end-plate connections in a 3D bare steel frame under fire loading: experimental study", Journal of Structural Fire Engineering, Vol. ahead-of-print No. ahead-of-print. https://doi.org/10.1108/JSFE-08-2021-0050

Daneshgar, M. A., & Mohammadi, M. (2018). Experimental and numerical investigation of the behavior of extended end plate connections. Engineering Structures, 170, 402-414. https://doi.org/10.1016/j.engstruct.2018.05.067

Alnahhal, R. A., & Al-Safary, J. H. (2016). Effect of end-plate thickness on the moment resistance of bolted connection with angles. Journal of Engineering and Development, 20(4), 1-17.

Adey, B.T. Grondin, G.Y. and Cheng J.J.R. (2000), “Cyclic loading of end plate moment connections”, Canadian Journal of Civil Engineering, 27(4), 638 – 701. https://doi.org/10.1139/l99-080

Hassan, R., Kishi, N., Chen, W.F. and Komuro, M. (1997), “Evaluation of rigidity of extended end plate connections”, Journal of Structural Engineering; 123(12), 1595 – 1602. https://doi.org/10.1061/(ASCE)0733-9445(1997)123:12(1595)

Grundy, P., Thomas, I.R., and Bennetts, I.D. (1980), "Beam-to-column moment connections", Journal Structure Engineering ASCE, 106(1), 313-330.

Bahaz, A., Amara, S., Jaspart, J.P. and Demonceau, J.F. (2018), “Analysis of the Behaviour of Semi Rigid Steel End Plate Connections”, MATEC Web of Conferences 149(02058), 1-6, https://doi.org/10.1051/matecconf/201814902058

Ioan, B. C., Cernescu, A. and Nicolae, N. (2021), “Design Method for End-Plate Bolted Connections, IOP Conference Series Materials Science and Engineering 1203(2), 022062, 1-11, https://doi.org/10.1088/1757-899X/1203/2/022062

Abidelah, A., Bouchair, A. and Kerdal, D.E. (2012), “Experimental and analytical behavior of bolted end-plate connections with or without stiffeners”, Journal of Constructional Steel Research, 76, 13-27. https://doi.org/10.1016/j.jcsr.2012.04.004

Shi, Y., Shi, G. and Wang, Y. (2006),” Experimental and theoretical analysis of the moment rotation behaviour of stiffened extended end plate connections”, Journal of Constructional Steel Research, 63(9), 1279–1293. https://doi.org/10.1016/j.jcsr.2006.11.008

Ismail, R.E.S., Fahmy, A.S., Khalifa, A.M. and Mohamed, Y.M. (2016), “Numerical study on ultimate behaviour of bolted end-plate steel connections”, Latin American Journal of Solids and Structures, 13, 1-22. https://doi.org/10.1590/1679-78251579

Dessouki, A.K., Youssef, A.H. and Ibrahim, M.M. (2013), “Behavior of I-beam bolted extended end-plate moment connections”, Ain Shams

Engineering Journal, 4, 685-699. http://dx.doi.org/10.1016/j.asej.2013.03.004

Chan, C.L., Khalid, Y.A., Sahari, B.B. and Hamouda, A.M.S. (2002), “Finite element analysis of corrugated web beams under bending”, Journal of Constructional Steel Research, 58(11), 1391-1406. https://doi.org/10.1016/S0143-974X(01)00075-X

Abbas, H.H. (2003), “Analysis and design of corrugated web I-girders for bridges using high performance steel”, Ph.D. dissertation, Lehigh Univ., Bethlehem, Pa.

Abbas, H.H., Richard, S.M., Robert, G.D., Kengo, A. and John, W.F.H. (2006), “Fatigue life of girders with trapezoidal corrugated webs”, Journal of Structural Engineering, 132(7), 1070 – 1078. https://doi.org/10.1061/(ASCE)0733-9445(2006)132:7(1070)

Moon, J., Yi, J., Choi, B.H. and Lee, H.E. (2009), “Shear strength and design of trapezoidally corrugated steel webs”, Journal of Constructional Steel Research, 65(5), 1198-1205. https://doi.org/10.1016/j.jcsr.2008.07.018

Khalid, Y.A., Chan, C.L., Sahari, B.B. and Hamouda, A.M.S. (2004), “Bending behaviour of corrugated beams”, Journal of Materials Processing Technology, 150(3), 242 – 254. https://doi.org/10.1016/j.jmatprotec.2004.02.042

Wang, X. (2003), Behavior of steel members with trapezoidally corrugated webs and tubular flanges under static loading, Research Project, Drexel University.

Imanpour, A., Mirghaderi, S. and Torabian, S. (2009), Experimental and numerical investigation of a new reduced beam section moment connection, behaviour of steel structures in seismic areas, CRC Press.

ElSabbagh, A., Sharaf, T., Nagy, S., ElGhandour, M. (2019), “Behavior of extended endplate bolted connections subjected to monotonic and cyclic loads” Engineering Structures, 190, 142-159

De’nan, F. and Hashim, N.S. (2011), “Study on bending behaviour of triangular web profile steel section by finite element analysis”, Applied Mechanics and Materials, 94, 1539-1544. https://doi.org/10.4028/www.scientific.net/AMM.94-96.1539

Özkılıç, Y. O. (2021), “Investigation of the effects of bolt diameter and endplate thickness on the capacity and failure modes of end-plated beam-to-column connections”, Research on Engineering Structures Materials, 7(3), 445-463.

Barmaki, S., Sheidaii, M. R. and Azizpour, O. (2020), Progressive collapse resistance of bolted extended end-plate moment connections, International Journal of Steel Structures, 20, 1165-1179 https://dx.doi.org/10.1007/s13296-020-00349-x

Md. Tahir, M., Sulaiman, A. and Saggaff, A. (2008) “Structural Behaviour of Trapezoidal Web Profiled Steel Beam Section using Partial Strength Connection” Electronic Journal of Structural Engineering, 8, 55-66 https://dx.doi.org/10.56748/ejse.8100

Ouh, M.H. (2009), Finite element analysis of semi rigid trapezoid web profiled beam to column extended end plate connection’, Research Project, Universiti Teknologi Malaysia.

Tai, W.Y. (2005), Finite element analysis of structural steelwork connection on minor axis using Lusas software, Research Report, Universiti Teknologi Malaysia.

Finite Element Analysis (FEA), LUSAS 13.57 (2004), LUSAS modeler user manual version 13, Surrey. United Kingdom: Finite Element Analysis Ltd

Nigel, D.B. (1995), “Aspects of frame sway design and ductility of composite endplate connections”, Ph.D. Dissertation, Department of Engineering University of Warwick, United Kingdom.

Saggaff, A. (2006), “Behaviour of composite partial strength connections with trapezoid web profiled steel section”, Ph.D. Dissertation, Faculty of Civil Engineering, Universiti Teknologi Malaysia.

Pan, J., Chen, S., Wang, Z. and Lu, H. (2018) “Initial rotational stiffness of minor-axis flush end-plate connections” Advances in Mechanical Engineering, 10(1), 1–9 https://dx.doi.org/10.1177/1687814017745397

Osman, A. A. and Mourad, S. A. (2021), “Performance of extended endplate bolted connections subjected to static and blast like loads” Journal of Engineering and Applied Science, 68(8), 1-25

Sathian, A and Geetha, P. R. (2020), “Study on behavior of extended endplate bolted connection subjected to cyclic loading” International Research Journal of Engineering and Technology, 7(8), 1872-1877

Yang, R. and Zhou, X. (2019), “Analysis of the Mechanical Behavior of Bolted Beam-Column Connections with Different Structural Forms”, Advances in Civil Engineering, 6, 1-11 https://dx.doi.org/10.1155/2019/1967253

Wang, Y., Wang, Z., Pan, J. and Wang, P. (2020), “Seismic Behavior of a Novel Blind Bolted Flush End-Plate Connection to Strengthened Concrete-Filled Steel Tube Columns”, Applied Sciences, 10(7), 1-26 https://dx.doi.org/10.3390/app10072517

Gholampour, A., Ghassemieh, M. and Jalalpour, M. (2014), “Numerical evaluation of the extended endplate moment connection subjected to cyclic loading”, Advances in Civil Engineering, 2(1), 35-43

Wang, C., Guo, Q., Zhang, W., & Liu, Y. (2020). Experimental study on fatigue behavior of anchor bolt connection in steel plate shear wall. Journal of Constructional Steel Research, 167, 106061. https://doi.org/10.1016/j.jcsr.2020.106061

Yin, M., Li, Q., Li, Z., Li, Y., & Li, G. (2021). Experimental study and numerical analysis on seismic behavior of steel shear walls with bolted connections. Journal of Constructional Steel Research, 184, 106849. https://doi.org/10.1016/j.jcsr.2021.106849

Disclaimer

The statements, opinions and data contained in all publications are solely those of the individual author(s) and contributor(s) and not of EJSEI and/or the editor(s). EJSEI and/or the editor(s) disclaim responsibility for any injury to people or property resulting from any ideas, methods, instructions or products referred to in the content.